

# Radio beam vorticity and orbital angular momentum

Bo Thidé<sup>1</sup>, Fabrizio Tamburini<sup>2</sup>, Elettra Mari<sup>3</sup>, Filippo Romanato<sup>4,5</sup> & Cesare Barbieri<sup>2</sup>

It has been known for a century that electromagnetic fields can transport not only energy and linear momentum but also angular momentum<sup>1,2</sup>. However, it was not until twenty years ago, with the discovery in laser optics of experimental techniques for the generation, detection and manipulation of photons in well-defined, pure orbital angular momentum (OAM) states<sup>3</sup>, that twisted light and its pertinent optical vorticity and phase singularities began to come into widespread use in science and technology<sup>4-6</sup>. We have now shown experimentally how OAM and vorticity can be readily imparted onto radio beams. Our results extend those of earlier experiments on angular momentum and vorticity in radio<sup>7-15</sup> in that we used a single antenna and reflector to directly generate twisted radio beams and verified that their topological properties agree with theoretical predictions. This opens the possibility to work with photon OAM at frequencies low enough to allow the use of antennas and digital signal processing, thus enabling software controlled experimentation also with first-order quantities, and not only second (and higher) order quantities as in optics-type experiments<sup>16</sup>. Since the OAM state space is infinite, our findings provide new tools for achieving high efficiency in radio communications and radar technology.

The total angular momentum around the origin  $\mathbf{x} = \mathbf{0}$  carried by an electromagnetic field ( $\mathbf{E}, \mathbf{B}$ ) in a volume  $V$  of free space is<sup>17-19</sup>  $\mathbf{J} = \epsilon_0 \int_V d^3x \mathbf{x} \times (\mathbf{E} \times \mathbf{B})$  where  $\epsilon_0$  is the free-space dielectric permittivity. For a beam where the fields fall off sufficiently rapidly with distance from the beam axis, the total angular momentum can be written  $\mathbf{J} = \mathbf{S} + \mathbf{L}$ , where the spin angular momentum  $\mathbf{S}$  is associated with the two states of wave polarisation and  $\mathbf{L}$  is the orbital angular momentum (OAM).

Optical vortices are phase defects<sup>20</sup> embedded in light beams that carry OAM<sup>21-23</sup>. Pure OAM state beams are characterized by a quantized topological charge  $\ell$ , which can take any integer value, corresponding to an OAM of  $\ell\hbar$  carried by each photon of the beam<sup>21</sup>. Also radio beams can be prepared in pure OAM states and superpositions thereof such that they contain vortices<sup>16</sup>.

Here we report the experimental confirmation of the generation and detection of a radio beam endowed with OAM and harbouring an electromagnetic vortex. The results were obtained in controlled laboratory experiments by employing the technique of letting a radio beam illuminate an approximately spiral-formed reflector, realised in 8 discontinuous steps and sampling the reflected radio beam in the far zone by using two identical dipole antennas.

If  $\lambda$  denotes the radio wavelength, and the reflector has  $N$  discrete jumps and a surface pitch  $\eta_\sigma$  (in the left-handed sense), the reflected beam will acquire the topological charge<sup>24</sup>

$$\ell = \frac{2\eta_\sigma}{\lambda} \left( \frac{N+1}{N} \right) \quad (1)$$

For  $\eta_\sigma = -6.22$  cm,  $\lambda = 12.49$  cm ( $\nu = 2.40$  GHz) and  $N = 8$  as in the experiments reported here, this formula predicts that the reflected radio beam had an effective OAM value of  $\ell \sim -1.12$ . According to the formula, a pure  $\ell = -1$  OAM eigenstate would have been achieved for  $\lambda = 13.99$  cm ( $\nu = 2.14$  GHz). However, the commercial 2.4–2.5 GHz LAN communications Yagi-Uda antenna that was used for generating the primary radio beam did not work satisfactorily at this frequency.

Our findings are summarized in Figures 1–3. Fig. 1a shows the prediction of the beam intensity distribution obtained in a numerical simulation, based on equation (1) for 2.40 GHz. Fig. 1b shows the outcome of the experiment. As is clearly seen, the existence of an annularly shaped intensity distribution around a central vortex eye, consistent with the existence of a vortex in the radio beam, was experimentally confirmed. The field intensity is weaker in the 2 o'clock direction, both in the simulation and the experiments. This is an effect of the non-integer value of  $\ell$  and of the corresponding imperfect phase matching over the full circle around the vortex eye. Figs. 2a–b show, respectively, the numerical and experimental results obtained when two receiving antennas were used, one held fixed at a maximum field point, and the other sampling different positions in a plane transverse to the radio beam axis. In this case the constructive and destructive interference of the two signals clearly result in a division of the map, along the diagonal, into two regions. Finally, we present in Fig. 3 an estimate of the comparison between the simulated and experimental phase map, interpolated from the one- and two-antenna measurements. Despite the unavoidable undersampling in the measurements and an ensuing limited accuracy, the phase behaviour, particularly the  $2\pi$  phase step in the 7 o'clock direction, clearly indicates that the beam carries OAM. We notice that the symmetry axis of the vortex and the phase singularity are both aligned with the mask gap direction of  $-45^\circ$  relative to the electric field polarization direction, as expected. The conclusion is that the experiment produced a radio-frequency vortex, in agreement with theory and numerical simulations.

The experimental verification of vorticity and OAM in radio means that a new frequency range has become available for fundamental as well as applied OAM-based experiments in disciplines ranging from relativistic astrophysics<sup>25</sup> and nanotechnology and biology<sup>26</sup>, to wireless communication with high spectral efficiency both classically<sup>15,27-29</sup> and quantum mechanically<sup>30,31</sup>. It also opens for the development of new radio and radar probing techniques, including spiral imaging<sup>32,33</sup>. It should also be emphasized that certain physical effects and observables associated with electromagnetic OAM, for instance electromagnetic torque, are stronger for lower frequencies than for higher<sup>7</sup>.

Perhaps the most striking practical applications of photon vorticity in optics and astronomy are super-resolution, where the Rayleigh limit can be overcome by at least one order of magni-

<sup>1</sup>Swedish Institute of Space Physics, Box 537, SE-75121 Uppsala, Sweden, EU.

<sup>2</sup>Department of Astronomy, University of Padova, vicolo dell'Osservatorio 3, IT-33122 Padova, Italy, EU.

<sup>3</sup>CISAS, Centro Interdipartimentale di Studi e Attività Spaziali G. Colombo, University of Padova, Via Venezia 15, IT-35131 Padova, Italy, EU.

<sup>4</sup>Department of Physics, University of Padova, via Marzolo, IT-35131, Padova, Italy, EU.

<sup>5</sup>LaNN, Laboratory for Nanofabrication of Nanodevices, Venetnanotech, via Stati Uniti 4, IT-35100 Padova, Italy, EU.

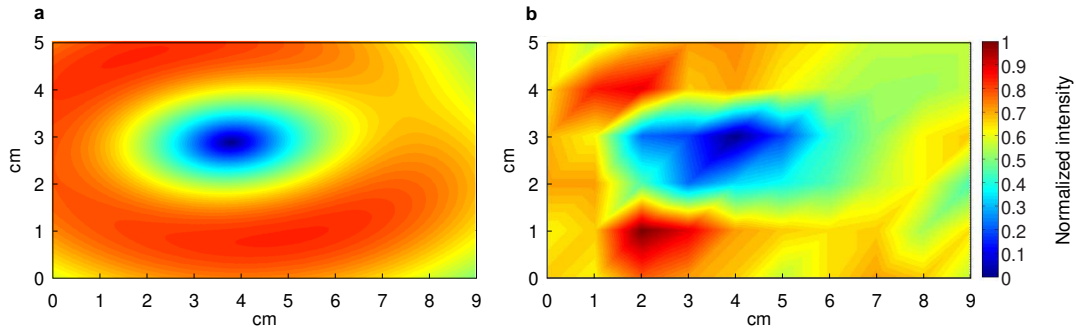


**Figure 1 | Single antenna signal.** **a**, The intensity of the radio beam in the far zone as obtained in numerical simulations. **b**, Experimental results obtained by probing the radio beam in a plane perpendicular to the beam

axis. The results exhibit a vortex singularity consistent with the numerical simulations.

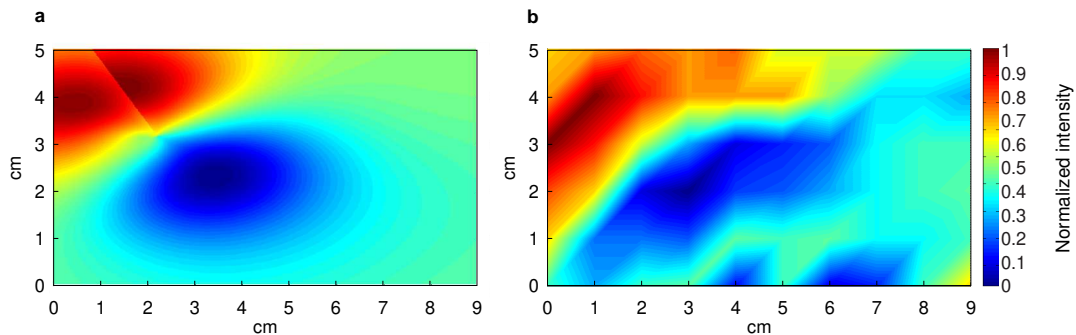


**Figure 2 | Sum of two antenna signals.** These plots show the intensity of the sum of the signal from one antenna at a maximum of the field, and the signal from a second antenna moved to different positions in a plane perpendicular to the beam axis. **a**, The numerical simulations. **b**, The

experimental results. The similarity of the patterns between simulations and experiments shows that the radio beam generated has topological signatures that are consistent with vorticity and OAM.

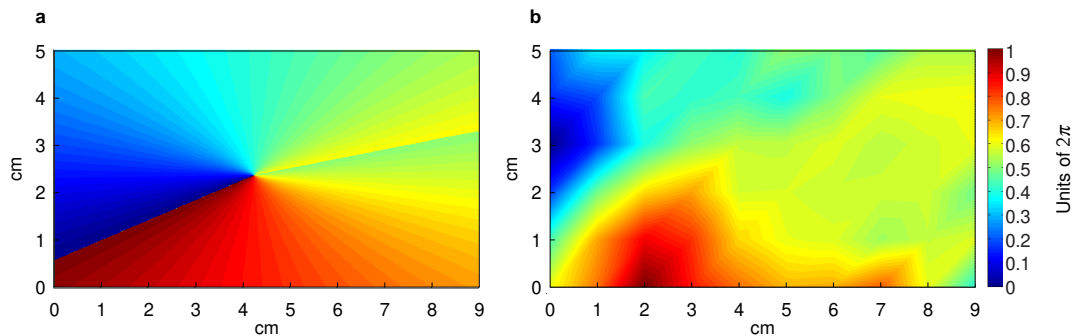


**Figure 3 | Phase map.** **a**, Simulated phase map of the radio beam in a far-zone plane perpendicular to the beam axis. The model predicts a  $2\pi$  phase step at  $-45^\circ$  (the 7 o'clock direction). **b**, Interpolated phase map,

based on measurements of the interference of two antenna signals as described above. The low lateral sampling resolution notwithstanding, the map clearly indicates the predicted  $2\pi$  phase step across the 7 o'clock line.

tude<sup>34</sup>, and highly efficient coronagraphy, where a contrast of up to  $10^{10}$  can be achieved<sup>24,35–41</sup>. In accordance with the trivial fact that Maxwell's equations are equally valid for optical and radio frequencies, our experiments show that the new OAM-based techniques developed and employed in optics can indeed be adapted to radio. Add to that the fact that electromagnetic orbital angular momentum for a large range of frequencies, including radio, can be used to reveal ionospheric, magnetospheric, interplanetary, and interstellar plasma turbulence<sup>32,42</sup> as well as rotating black

holes<sup>25</sup> and one realises that we are likely to witness a very rapid development in the space sciences.

## METHODS SUMMARY

The experiments were performed in the anechoic antenna chamber at the Ångström Laboratory of the Uppsala University, Uppsala, Sweden. The chamber is electromagnetically as well as acoustically/vibrationally shielded from the outside world. The experiments were performed at 2.4 gigahertz (12.49 cm wavelength) with a resonant 7-element Yagi-Uda an-

tenna fed from a signal generator with a continuous 0.01 watt signal. The radio beam was reflected off a discrete eight-step approximation of a spiral reflector designed for a total  $2\pi$  phase shift, mimicking an ideal, smooth spiral reflector. The reflected, twisted radio beam was probed with two resonant electric dipole antennas, on axis in the far zone, 7 metres ( $\sim 55\lambda$ ) away from the non-focusing reflector. One of the receiving antennas was held at a fixed position whereas the other was moved around to sample the signal at different fixed grid points in the one and the same plane perpendicular to the radio beam axis. By making a simultaneous measurement of the two antenna signals, the absolute amplitude and the relative phase of the electric field of the antenna beam could be estimated.

1. Poynting, J. H. The wave motion of a revolving shaft, and a suggestion as to the angular momentum in a beam of circularly polarised light. *Proc. Roy. Soc. London A* **82**, 560–567 (1909).
2. Abraham, M. Der Drehimpuls des Lichtes. *Physik. Zeitschr.* **XV**, 914–918 (1914).
3. Beijersbergen, M. W., Coerwinkel, R. P. C., Kristensen, M. & Woerdman, J. P. Helical-wavefront laser beams produced with a spiral phaseplate. *Opt. Commun.* **112**, 321–327 (1994).
4. Molina-Terriza, G., Torres, J. P. & Torner, L. Twisted photons. *Nature Phys.* **3**, 305–310 (2007).
5. Franke-Arnold, S., Allen, L. & Padgett, M. Advances in optical angular momentum. *Laser & Photon. Rev.* **2**, 299–313 (2008).
6. Torres, J. P. & Torner, L. *Twisted Photons: Applications of Light With Orbital Angular Momentum* (Wiley-Vch Verlag, John Wiley and Sons, Weinheim, DE, 2011). ISBN: 978-3-527-40907-5.
7. Carrara, N. Torque and angular momentum of centimetre electromagnetic waves. *Nature* **164**, 882–884 (1949).
8. Carrara, N. Coppia e momento angolare della radiazione. *Nuov. Cim.* **VI**, 50–56 (1949).
9. di Francia, G. T. On a macroscopic measurement of the spin of electromagnetic radiation. *Nuov. Cim.* **6**, 150–167 (1957).
10. Allen, P. J. A radiation torque experiment. *Am. J. Phys.* **34**, 1185–1192 (1966).
11. Carusotto, S., Fornaca, G. & Polacco, E. Radiation beats and rotating systems. *Nuov. Cim.* **53**, 87–97 (1968).
12. Hajnal, J. V. Observations of singularities in the electric and magnetic fields of freely propagating microwaves. *Proc. Roy. Soc. London A* **430**, 413–421 (1990).
13. Kristensen, M. & Woerdman, J. P. Is photon angular momentum conserved in a dielectric medium? *Phys. Rev. Lett.* **74**, 2171–2171 (1994).
14. Courtial, J., Robertson, D. A., Dholakia, K., Allen, L. & Padgett, M. J. Rotational frequency shift of a light beam. *Phys. Rev. Lett.* **81**, 4828–4830 (1998).
15. Jiang, Y., He, Y. & Li, F. Wireless communications using millimeter-wave beams carrying orbital angular momentum. In *Communications and Mobile Computing, 2009. CMC '09. WRI International Conference on*, vol. 1, 495–500 (Kunming, Yunnan, China, 2009).
16. Thidé, B. *et al.* Utilization of photon orbital angular momentum in the low-frequency radio domain. *Phys. Rev. Lett.* **99**, 087701(4) (2007).
17. Schwinger, J., DeRaad, L. L., Jr., Milton, K. A. & Tsai, W. *Classical Electrodynamics* (Perseus Books, Reading, MA, USA, 1998). ISBN 0-7382-0056-5.
18. Jackson, J. D. *Classical Electrodynamics* (Wiley & Sons, New York, NY, USA, 1999), third edn. ISBN 0-471-30932-X.
19. Thidé, B. *Electromagnetic Field Theory* (Dover Publications, Inc., Mineola, NY, USA, 2011), 2nd edn. URL <http://www.plasma.uu.se/CED/Book>. ISBN: 978-0-486-4773-2.
20. Nye, J. F. & Berry, M. V. Dislocations in wave trains. *Proc. Roy. Soc. London A* **336**, 165–190 (1974).
21. Allen, L., Beijersbergen, M. W., Spreeuw, R. J. C. & Woerdman, J. P. Optical angular momentum of light and the transformation of Laguerre-Gauss laser modes. *Phys. Rev. A* **45**, 8185–8189 (1992).
22. Padgett, M., Arlt, J., Simpson, N. & Allen, L. An experiment to observe the intensity and phase structure of Laguerre-Gaussian laser modes. *Am. J. Phys.* **64**, 77–82 (1996).
23. Padgett, M. J. & Allen, L. The Poynting vector in Laguerre-Gaussian laser modes. *Opt. Commun.* **121**, 36–40 (1995).
24. Mari, E., Anzolin, G., Tamburini, F. *et al.* Fabrication and testing of  $l = 2$  optical vortex phase masks for coronagraphy. *Opt. Express* **18**, 2339–2344 (2010).
25. Tamburini, F., Thidé, B., Molina-Terriza, G. & Anzolin, G. Twisting of light around rotating black holes. *Nature Phys.* **in press** (2011). Doi: 10.1038/NPHYS1907.
26. Grier, D. G. A revolution in optical manipulation. *Nature* **424**, 810–816 (2003).
27. Gibson, G. *et al.* Free-space information transfer using light beams carrying orbital angular momentum. *Opt. Express* **12**, 5448–5456 (2004).
28. Gibson, G., Courtial, J., Barnett, M. V. S. & Franke-Arnold, S. Increasing the data density of free-space optical communications using orbital angular momentum. In Rickling, J. C. & Voetz, D. G. (eds.) *Free-Space Laser Communications IV*, vol. 5550 of *Proceedings of SPIE*, 367–373 (Denver, CO, USA, 2004). URL <http://link.aip.org/link/?PSI/5550/367/1&Agg=doi>.
29. Čelechovský, R. & Bouchal, Z. Optical implementation of the vortex information channel. *New J. Phys.* **9**, 328 (2007).
30. Pors, J. B. *et al.* Shannon dimensionality of quantum channels and its application to photon entanglement. *Phys. Rev. Lett.* **101**, 120502 (2008).
31. Barreiro, J. T., Wei, T.-C. & Kwiat, P. W. Beating the channel capacity limit for linear photonic superdense coding. *Nature Phys.* **4**, 282–286 (2008).
32. Thidé, B. Nonlinear physics of the ionosphere and LOIS/LOFAR. *Plasma Phys. Contr. Fusion* **49**, B103–B107 (2007).
33. Molina-Terriza, G., Rebane, L., Torres, J. P., Torner, L. & Carrasco, S. Probing canonical geometrical objects by digital spiral imaging. *J. Eur. Opt. Soc.* **2**, 07014(6) (2007).
34. Tamburini, F., Anzolin, G., Umbriaco, G., Bianchini, A. & Barbieri, C. Overcoming the Rayleigh criterion limit with optical vortices. *Phys. Rev. Lett.* **97**, 163903(4) (2006).
35. Swartzlander, G. A., Jr. Peering into darkness with a vortex filter. *Opt. Lett.* **26**, 497–499 (2001).
36. Lee, J. H., Foo, G., Johnson, E. G. & Swartzlander, G. A., Jr. Experimental verification of an optical vortex coronagraph. *Phys. Rev. Lett.* **97**, 053901(4) (2006).
37. Swartzlander, G. A., Jr. *et al.* Astronomical demonstration of an optical vortex coronagraph. *Opt. Express* **16**, 10200–10207 (2008).
38. Anzolin, G., Tamburini, F., Bianchini, A., Umbriaco, G. & Barbieri, C. Optical vortices with starlight. *Astron. Astrophys.* **488**, 1159–1165 (2008).
39. Barbieri, C. *et al.* Light's orbital angular momentum and optical vortices for astronomical coronagraphy from ground and space telescopes. *Earth Moon Plan.* **105**, 283–288 (2009).
40. Mawet, D. *et al.* The vector vortex coronagraph: Laboratory results and first light at Palomar observatory. *Astrophys. J.* **709**, 53–57 (2010).
41. Serabyn, E., Mawet, D. & Burruss, R. An image of an exoplanet separated by two diffraction beamwidths from a star. *Nature* **464**, 1018–1020 (2010).
42. Tamburini, F., Sponselli, A., Thidé, B. & Mendonça, J. T. Photon orbital angular momentum and mass in a plasma vortex. *Europhys. Lett.* **90**, 45001 (2010).

**Acknowledgements** B. T. acknowledges the financial support from the Swedish Research Council (VR) and the hospitality of the Nordic Institute for Theoretical Physics (NORDITA), Stockholm. F. T. and E. M. gratefully acknowledge the support from the Vortici e Frequenze group, Orseolo Restauri, CARIPARO Foundation within the 2006 and 2008 Program of Excellence, and the kind hospitality of Uppsala University, The Ångström Laboratory antenna chamber was funded by a grant from the Knut and Alice Wallenberg Foundation. We thank Anders Rydberg and Jonas Bothén for technical assistance.